Journal of Computers Vol. 29 No. 2, 2018, pp. 86-95
doi:10.3966/199115992018042902009

Research of AC Motor Vector Control System Voltage Model Adaptive Internal Model Control

Bo Hu[1], Lun Xie[1*], Lei Zhang[1], Fuji Ren[2], Dan Li[1], Zhi-liang Wang[1]

[1] School of Computer and Communication Engineering, University of Science and Technology Beijing, Beijing, 100083, China
xielun@ustb.edu.cn

[2] Affective Computing and Advanced Intelligent Machines Key Laboratory, HeFei University of Technology, Hefei, 230009, China

Received 24 July 2017; Revised 19 September 2017; Accepted 19 October 2017

Abstract. In latest motor control area, traditional voltage model is affected by variation of stator resistance and pure integration element of back electromotive force under the circumstance of low speed, whose effects would easily cause observation errors and lower motor speed control precision. Adaptive internal model control (AIMC for short) structure can adapt to stator resistance parameters variation and improve control precision. Cascaded Low pass filter (LPF for short) with compensation structure was proposed to revise amplitude and phase of observed flux linkage. The paper proposed the theory of AIMC and LPC, the structure would improve the accuracy of flux observer. At the same time, disturbance eliminating with compensation structure was put forward to improve the system anti-interference ability. Finally, PSIM 9.0.was used to build and simulate AC-DC-AC synchronous machine vector control system. Experiment results showed that the improved voltage model can effectively restrain the effects of stator resistance parameters variation. At the same time, precision of flux observer was effectively improved. Anti-interference ability of system was enhanced with nice tracking performance and robustness.

Keywords: adaptive internal model control, cascaded LPF with compensation structure, disturbance eliminating, flux observer, voltage model

1 Introduction

Because traditional high-power AC synchronous motor system has good control performance and high precision, it was widely used in hot continuous rolling [1].Voltage model act as an important approach in flux observation, it's the key factor to realize vector control. Unfortunately, voltage model not only affected by variation of stator resistance, but also pure integration element of back electromotive force, this would lead depend too much on motor parameters and low flux observation accuracy. To reduce the dependency of controlled object, this paper combined internal model control with model reference adaptive to design voltage model adaptive internal model control (AIMC) [2] system. Pure integration element of back electromotive force is easy to result in DC bias and integral saturation. Flux observer's results, including amplitude and phase, will deviate gravely from the true value. By calculation, the flux observer error compensation can be realized by cascade low-pass filters in accordance with certain conditions. In order to improve the system anti-interference ability, this paper designed disturbance eliminating with compensation structure to eliminate inner disturbance with known model and external disturbance to make sure system work stable and reliable. At last, we built and simulated AC-DC-AC synchronous motor vector control system in PSIM 9.0 to verify the performance of proposed system.

* Corresponding Author

2 Design of System

2.1 Voltage Model Direct Adaptive Parameter Estimation

Design of internal model control (IMC) usually parallel object model and controlled object and let controller approximate to object model's dynamic inverse [3]. The closer object model and controlled object, the more accurate IMC is, the more can it reflect controlled object. Traditional voltage model (is shown in Fig. 1.) is designed in this way. Compared with parameter integrated decision of traditional PID control, IMC has advantages such as fewer parameter, simple structure and convenient to adjust online [4]. So, IMC is widely used in control system. Zitek, P proposed a kind of stable fault detection system by combing IMC with artificial neural network (ANNs). This system can predict and realizea very small error in a short time [5]. Shihabudheen, K.V. proposed a kind of extreme learning adaptive fuzzy neural prediction algorithm which optimized generalization ability and trajectory tracking performance [6]. Tomas and Pajchrowski put forward a method that use improved elastic feedback to train neural model's inverse online to realize control when motor parameters change [7]. This paper designed adaptive parameter estimation structure firstly.

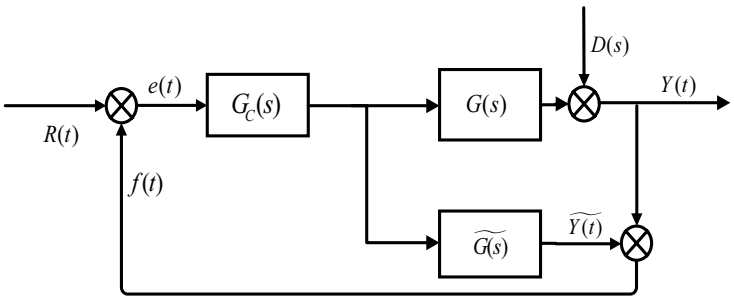

Fig. 1. Traditional voltage model

In the air gap flux oriented vector control theory, AC synchronous motor voltage model equation is,

$$\begin{cases} \psi_{\delta\alpha} = \int E_\alpha dt = \int (u_{s\alpha} - R_s i_{s\alpha})dt - L_{sl} i_{s\alpha} \\ \psi_{\delta\beta} = \int E_\beta dt = \int (u_{s\beta} - R_s i_{s\beta})dt - L_{sl} i_{s\beta} \end{cases}$$

In the formula, $u_{s\alpha}$, $u_{s\beta}$ stands for $\alpha\beta$ axis component of stator voltage respectively, $i_{s\alpha}$, $i_{s\beta}$ stands for $\alpha\beta$ axis component of stator current respectively, R_s stands for statorresistance, L_{sl} stands for stator winding leakage inductances, $\psi_{\delta\alpha}$, $\psi_{\delta\beta}$ stands for $\alpha\beta$ axis component of flux.

After Laplace transform, $\begin{cases} E_\alpha(s) = u_{s\alpha}(s) - (R_s + sL_{sl}) i_{s\alpha}(s) \\ E_\beta(s) = u_{s\beta}(s) - (R_s + sL_{sl}) i_{s\beta}(s) \end{cases}$ **(1)**

Assuming that $\boldsymbol{E(s)} = \begin{bmatrix} \boldsymbol{E_\alpha(s) - u_{s\alpha}(s)} \\ \boldsymbol{E_\beta(s) - u_{s\beta}(s)} \end{bmatrix}$

$$\boldsymbol{G(s)} = \begin{bmatrix} \boldsymbol{-R_s - sL_{sl}} & \boldsymbol{0} \\ \boldsymbol{0} & \boldsymbol{-R_s - sL_{sl}} \end{bmatrix}^{-1}, \quad \boldsymbol{Y(s)} = \begin{bmatrix} \boldsymbol{i_{s\alpha}(s)} \\ \boldsymbol{i_{s\beta}(s)} \end{bmatrix},$$

so (1) was converted to $Y(s) = G(s)E(s)$ **(2)**

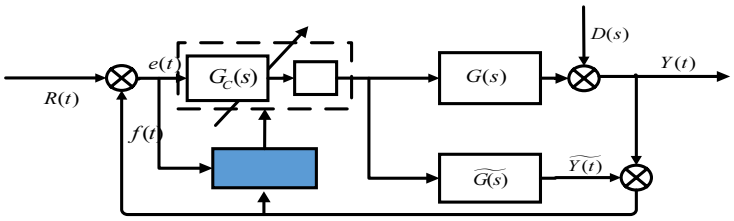

Fig. 2. Voltage model with adaptive parameter estimator

Indirect adaptive parameter estimator usually use least square to adjust system parameters online to increase the control accuracy of model [8]. But its dynamic performance is not as well as direct adaptive parameter estimator. To guarantee dynamic performance, we adopt the latter. We added filter $Q(s)=\frac{1}{(1+\alpha s)^n}I$ (α is the only parameter need to adjust) to make sure physically realizable and robustness. As the controlled object is stable, we can assumption feed-forward low-pass filter $Q(s)$ as a first order system, means $Q(s)=\frac{\alpha}{s+\alpha}I$ (α is adjustable).

$$G_C(s)=G^{-1}(s)Q(s)\ \ \widetilde{G_C}(s)=\widetilde{G^{-1}}(s)Q(s) \tag{3}$$

Obtained, $\boldsymbol{G_C(s)=\begin{bmatrix} -R_s - sL_{sl} & 0 \\ 0 & -R_s - sL_{sl} \end{bmatrix} Q(s)}$

Firstly, we need to choose smaller α to guarantee better dynamic performance. Increase α adaptively while model error seriously affected stability of system. Through experiments, we obtained good performance when choose adaptive law as $\alpha_1=\alpha_0(1+1.45)$.

1.2 Voltage Model Adaptive Internal Controller

Different from robust control, the basis of adaptive internal model control is model and parameter estimation. AIMC doesn't need to know information such as disturbance boundary and time-varying parameters in advance, but adapt to system parameter changes in real time by measurement [9]. In the design of internal model controller, the more accurate object model and inverse model is, the better control effect is. Although model parameters can be obtained from history data, system characteristics may change with external interference, which means it's hard to get accurate model. On the contrary, model reference adaptive control has certain adaptive ability. It can get rid of disadvantages of model changes over time. From this point, this paper combined internal control with model reference adaptive control to design voltage model adaptive internal controller and adaptive law [10]. On the other hand, disturbance eliminating with compensation structure was designed to increase anti-interference ability. The whole structure is as follow.

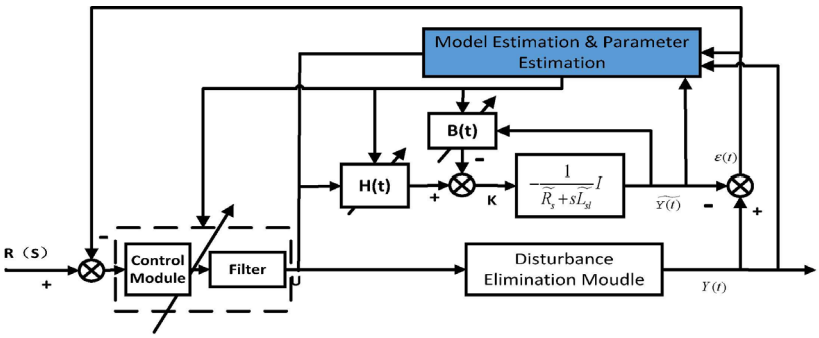

Fig. 3. Voltage model adaptive internal controller

1.3 Model Estimator of Adaptive Internal Model

Voltage model direct adaptive parameter estimation has been introduced in part 2.1,then we will design model estimation in voltage model adaptive internal controller. According to synchronous motor voltage model equation, the differential equation of controlled object and object model is as follow.

$$\dot{Y}(t) = AY(t) + BE(t) \quad \dot{\tilde{Y}}(t) = \tilde{A}\tilde{Y}(t) + \tilde{B}k(t) \tag{4}$$

Where $\boldsymbol{A} = \begin{bmatrix} -\frac{\boldsymbol{R_s}}{\boldsymbol{L_{sl}}} & \boldsymbol{0} \\ \boldsymbol{0} & -\frac{\boldsymbol{R_s}}{\boldsymbol{L_{sl}}} \end{bmatrix}$ $\boldsymbol{B} = \begin{bmatrix} -\frac{\boldsymbol{1}}{\boldsymbol{L_{sl}}} & \boldsymbol{0} \\ \boldsymbol{0} & -\frac{\boldsymbol{1}}{\boldsymbol{L_{sl}}} \end{bmatrix}$ $\boldsymbol{Y(t)} = \begin{bmatrix} \boldsymbol{i_{s\alpha}} \\ \boldsymbol{i_{s\beta}} \end{bmatrix}$ $\boldsymbol{E(t)} = \begin{bmatrix} \boldsymbol{E_\alpha - u_{s\alpha}} \\ \boldsymbol{E_\beta - u_{s\beta}} \end{bmatrix}$,

$\tilde{\boldsymbol{A}} = \begin{bmatrix} -\frac{\widetilde{\boldsymbol{R_s}}}{\widetilde{\boldsymbol{L_{sl}}}} & \boldsymbol{0} \\ \boldsymbol{0} & -\frac{\widetilde{\boldsymbol{R_s}}}{\widetilde{\boldsymbol{L_{sl}}}} \end{bmatrix}$ $\tilde{\boldsymbol{B}} = \begin{bmatrix} -\frac{\boldsymbol{1}}{\widetilde{\boldsymbol{L_{sl}}}} & \boldsymbol{0} \\ \boldsymbol{0} & -\frac{\boldsymbol{1}}{\widetilde{\boldsymbol{L_{sl}}}} \end{bmatrix}$ $\tilde{\boldsymbol{Y}}\boldsymbol{(t)} = \begin{bmatrix} \widetilde{\boldsymbol{i_{s\alpha}}} \\ \widetilde{\boldsymbol{i_{s\beta}}} \end{bmatrix}$ $\tilde{\boldsymbol{E}}\boldsymbol{(t)} = \begin{bmatrix} \tilde{\boldsymbol{E}}_\alpha - \tilde{\boldsymbol{u}}_{s\alpha} \\ \tilde{\boldsymbol{E}}_\beta - \tilde{\boldsymbol{u}}_{s\beta} \end{bmatrix}$

$\tilde{Y}(t)$, $\tilde{A}$, $\tilde{B}$, $\tilde{E}(t)$ is used to distinguish from controlled object.

Input of reference model $k(t) = H(t)U(t) - B(t)\tilde{Y}(t)$, where $H(t)$ and $B(t)$ stands for feed-forward and feed-back, they are adjustable.

$$\dot{\tilde{Y}}(t) = \tilde{A}\tilde{Y}(t) + \tilde{B}(H(t)U(t) - B(t)\tilde{Y}(t)) = (\tilde{A} - \tilde{B}B(t))\tilde{Y}(t) + \tilde{B}H(t)U(t) \quad \boldsymbol{U(t)} = \begin{bmatrix} \boldsymbol{E_\alpha - u_{s\alpha}} \\ \boldsymbol{E_\beta - u_{s\beta}} \end{bmatrix} \quad Q\varepsilon(t) = Y(t) - \tilde{Y}(t)$$

$$\because \dot{\varepsilon}(t) = \dot{Y}(t) - \dot{\tilde{Y}}(t) = A\varepsilon(t) + P\tilde{Y}(t) + QU(t) \tag{5}$$

$$\boldsymbol{P = A - \tilde{A} + \tilde{B}B(t)} = \begin{bmatrix} -\frac{\boldsymbol{R_s}}{\boldsymbol{L_{sl}}} + \frac{\widetilde{\boldsymbol{R_s}}}{\widetilde{\boldsymbol{L_{sl}}}} & \boldsymbol{0} \\ \boldsymbol{0} & -\frac{\boldsymbol{R_s}}{\boldsymbol{L_{sl}}} + \frac{\widetilde{\boldsymbol{R_s}}}{\widetilde{\boldsymbol{L_{sl}}}} \end{bmatrix} + \begin{bmatrix} \frac{\boldsymbol{-1}}{\widetilde{\boldsymbol{L_{sl}}}} & \boldsymbol{0} \\ \boldsymbol{0} & -\frac{\boldsymbol{1}}{\widetilde{\boldsymbol{L_{sl}}}} \end{bmatrix} \boldsymbol{B(t)}$$

$$\boldsymbol{Q = B - \tilde{B}H(t)} = \begin{pmatrix} -\frac{\boldsymbol{1}}{\boldsymbol{L_{sl}}} & \boldsymbol{0} \\ \boldsymbol{0} & -\frac{\boldsymbol{1}}{\boldsymbol{L_{sl}}} \end{pmatrix} + \begin{pmatrix} \frac{\boldsymbol{1}}{\widetilde{\boldsymbol{L_{sl}}}} & \boldsymbol{0} \\ \boldsymbol{0} & \frac{\boldsymbol{1}}{\widetilde{\boldsymbol{L_{sl}}}} \end{pmatrix} \boldsymbol{H(t)}$$

$$\text{If } \varphi^{\mathrm{T}} = \begin{pmatrix} P & Q \end{pmatrix}, \tau = \begin{pmatrix} \tilde{Y}(t) & U(t) \end{pmatrix}^{\mathrm{T}}, \ \dot{\varepsilon}(t) == A\varepsilon(t) + \varphi^T\tau \tag{6}$$

Then we design adaptive law based on Lyapunov stability theorem, which is based on the point of energy stability. It can avoid solving differential equations. By choosing proper Lyapunov function, stable control law in form of mathematic analysis can be obtained [11]. If the designed function satisfy the first Lyapunov theorem, which means $V(y,t) > 0$ and $\dot{V}(y,t) < 0$, then the origin is asymptotically stable [12]. In order to make Lyapunov function definitely positive.

$$V(y,t) = \frac{1}{2}\left(\varepsilon^T E_1 \varepsilon + \varphi^T E_2 \varphi\right) \tag{7}$$

E_1, E_2 is unit matrix, assuming balance point is $\varepsilon = \varphi^{\mathrm{T}} = 0$.

$$\dot{V}(y,t)=\frac{1}{2}\left(\dot{\varepsilon}^{T}E_1\varepsilon+\varepsilon^{T}E_1\dot{\varepsilon}+\dot{\varphi}^{T}E_2\varphi+\varphi^{T}E_2\dot{\varphi}\right)$$

$$=\frac{1}{2}(\varepsilon^{T}A^{T}E_1\varepsilon+\tau^{T}\varphi E_1\varepsilon+\varepsilon^{T}E_1A\varepsilon+\varepsilon^{T}E_1\varphi^{T}\tau+\dot{\varphi}^{T}E_2\varphi+\varphi^{T}E_2\dot{\varphi}) \quad \textbf{(8)}$$

$$=\frac{1}{2}\varepsilon^{T}(A^{T}E_1+E_1A)\varepsilon+\frac{1}{2}(\tau^{T}\varphi E_1\varepsilon+\varepsilon^{T}E_1\varphi^{T}\tau+\dot{\varphi}^{T}E_2\varphi+\varphi^{T}E_2\dot{\varphi})$$

$$\boldsymbol{QA^{T}E_1+E_1A}=\begin{pmatrix}-\dfrac{2R_s}{L_{sl}} & 0\\ 0 & -\dfrac{2R_s}{L_{sl}}\end{pmatrix}$$

So $\frac{1}{2}\varepsilon^{\mathrm{T}}(A^{\mathrm{T}}E_1+E_1A)\varepsilon$ is negative definite.

Only need to prove (9) can satisfy conditions.

$$\frac{1}{2}(\tau^{T}\varphi E_1\varepsilon+\varepsilon^{T}E_1\varphi^{T}\tau+\dot{\varphi}^{T}E_2\varphi+\varphi^{T}E_2\dot{\varphi})=0 \quad \textbf{(9)}$$

After calculate, $\tau^{\mathrm{T}}\varphi E_1\varepsilon=\varepsilon^{\mathrm{T}}E_1\varphi^{\mathrm{T}}\tau=(\tilde{Y}^{\mathrm{T}}P+U^{\mathrm{T}}Q)\varepsilon$, $\dot{\varphi}^{\mathrm{T}}E_2\varphi=\varphi^{\mathrm{T}}E_2\dot{\varphi}=\dot{P}P+\dot{Q}Q$

(9) was transformed as $(\tilde{Y}^{\mathrm{T}}P+U^{\mathrm{T}}Q)\varepsilon+\dot{P}P+\dot{Q}Q=(\tilde{Y}^{\mathrm{T}}\varepsilon+\dot{P})P+(U^{\mathrm{T}}\varepsilon+\dot{Q})Q=0$ So $(\tilde{Y}^{\mathrm{T}}\varepsilon+\dot{P})P=0$, $(U^{\mathrm{T}}\varepsilon+\dot{Q})Q=0$

$\dot{P}=-\tilde{Y}^{\mathrm{T}}\varepsilon$, $\dot{Q}=-U^{\mathrm{T}}\varepsilon$

$\because \dot{P}=\tilde{B}\dot{B}(t)$ $\dot{Q}=-\tilde{B}\dot{H}(t)$,

The adaptive law is $\dot{B}(t)=-\frac{1}{\tilde{B}}\tilde{Y}^{\mathrm{T}}\varepsilon$, $\dot{H}(t)=\frac{1}{\tilde{B}}U^{\mathrm{T}}\varepsilon$

Now, $V(y,t)>0$, $\dot{V}(y,t)<0$,system is asymptotically stable at origin.

1.4 Disturbance Eliminating with Compensation Structure

Motor disturbance is inevitable and may decrease the traceability [13]. Traditional adaptive control gives both output and disturbance to input to improve system performance and eliminate interference. Disturbance eliminating effect have to compromise. Adaptive inverse control'sdynamic response and disturbance eliminating control is carried out separately, this can guarantee better dynamic performance and do its best to eliminate disturbance [14]. Besides, if the inner disturbance model of system is known, such as n times harmonic, compensation measures can be adopted to eliminate it. In internal model control system, controlled object and object model have the same input make object model convenient to close to controlled object. Dynamic response generated by inner disturbance was added to the inverse of model, whose output was given to the actual input. Then the input was fixed. The inner and external disturbance was eliminated eventually.

Assuming that $T(s)$ include inner disturbance **M(s)**, according to (1)

$$\boldsymbol{G(s)=\widetilde{G}(s)=}\begin{bmatrix}\boldsymbol{-R_s-sL_{sl}} & \boldsymbol{0}\\ \boldsymbol{0} & \boldsymbol{-R_s-sL_{sl}}\end{bmatrix}^{-1} \qquad \boldsymbol{G^{-1}(s)=}\begin{bmatrix}\boldsymbol{-R_s-sL_{sl}} & \boldsymbol{0}\\ \boldsymbol{0} & \boldsymbol{-R_s-sL_{sl}}\end{bmatrix}$$

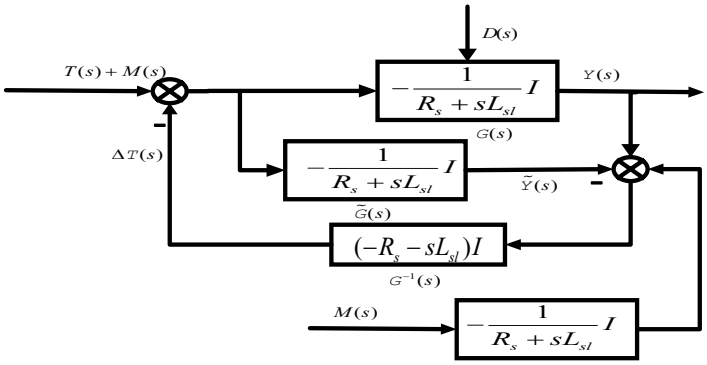

Fig. 4. Disturbance eliminate with compensation structure

The difference between controlled object and object model is

$$\begin{aligned}\varepsilon(s) &= Y(s) - \tilde{Y}(s) = (T(s) + M(s))G(s) + \\ &D(s)G(s) - (T(s) + M(s))\tilde{G}(s) = D(s)G(s)\end{aligned} \tag{10}$$

$$\Delta T(s) = (\varepsilon(s) + M(s) \cdot G(s))G^{-1}(s) = D(s) + M(s)$$

Fixed input is $T_R(s) = T(s) + M(s) - \Delta T(s) = T(s) - D(s)$

Actual output of controlled model after fix.

$$Y_R(s) = T_R(s)G(s) + D(s)G(s) = T(s)G(s)$$

Both $M(s)$ and $D(s)$ were eliminated.

1.5 Cascade Low-Pass Filter (LPF) with Compensation Structure

Due to the pure integral link in voltage model, which usually causes DC bias, integral saturation and flux waveforms shift seriously [15]. This urgent problem would lead to a bigger error. This phenomenon always become worse when met electromagnetic interference and sensor error [16]. Improved voltage model is proposed in this paper, voltage and current item would be processed respectively, and finally compensate amplitude and phase [17]. The structure is shown in Fig. 5.

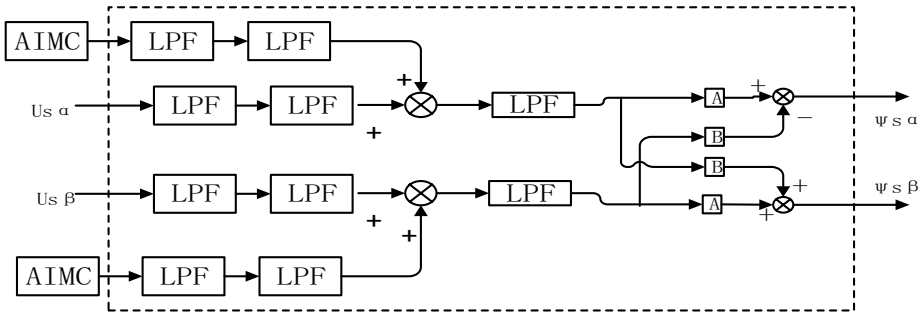

Fig. 5. Cascade Low-Pass Filter (LPF) with compensation structure

Cut-off frequency is ω_1 、 ω_2 、 ω_3, compensation quantity is X_1 、 X_2 、 X_3 respectively.

$$\frac{1}{s+\omega_1}X_1 = \frac{1}{s} \Rightarrow X_1 = 1 - j\frac{\omega_1}{\omega_e}, \frac{1}{s+\omega_2}X_2 = 1 \Rightarrow X_2 = \omega_2 + j\omega_e \frac{1}{s+\omega_3}X_3 = 1 \Rightarrow X_3 = \omega_3 + j\omega_e$$

Total compensation quantity, $X = X_1X_2X_3$

Because $\psi_{s\alpha} + j\psi_{s\beta} = (\psi^*_{s\alpha} + j\psi^*_{s\beta})X$

$$\begin{cases} \psi_{s\alpha} = A\psi^*_{s\alpha} - B\psi^*_{s\beta} \\ \psi_{s\beta} = B\psi^*_{s\alpha} + A\psi^*_{s\beta} \end{cases} \tag{11}$$

Where $A = \omega_1\omega_2 + \omega_1\omega_3 + \omega_2\omega_3 - \omega_e^2$, $B = \omega_2\omega_e + \omega_3\omega_e + \omega_1\omega_e - \dfrac{\omega_1\omega_2\omega_3}{\omega_e}$

Cascade two LPF after voltage and current item and one LPF in major loop can deal with voltage and current item respectively. Only need to satisfy one condition: amplitude and phase errors keep the same. The relationship of cut-off frequency is shown in formula (12). The cut-off frequency of LPF cascaded after current item is ω_{i1} 、 ω_{i2}, corresponding compensation quantity is X_{i1} 、 X_{i2}. The cut-off frequency of LPF cascaded after voltage item is ω_{u1} 、 ω_{u2}, corresponding compensation quantity is X_{u1} 、 X_{u2}.

$$X_{i1}X_{i2} = X_{u1}X_{u2} \Rightarrow \begin{cases} \omega_{i1}\omega_{i2} = \omega_{u1}\omega_{u2} \\ \omega_{i1} + \omega_{i2} = \omega_{u1} + \omega_{u2} \end{cases} \tag{12}$$

So can we deal with voltage and current items respectively.

2 Simulation Results

This paper simulated in PSIM 9.0, which is a software applied in the field of power electronics and motor control. Semiconductor switching devices in PSIM 9.0 are ideal model. PSIM 9.0 uses efficient algorithms to overcome the disadvantage that simulation time is too long compared with other software. At the same time, it greatly reduced the design cycle. This paper use AC-DC-AC synchronous motor vector control system, motor parameter is shown in Table 1.

Table 1. Motor parameters

Rated Power	Rated Voltage	Rated Current	Rs	Lsl	Pole-pairs Number	Speed
2500Kw	1650V	980A	0.0244Ω	2.52mH	4	100 r/min

The whole structure is as follow.

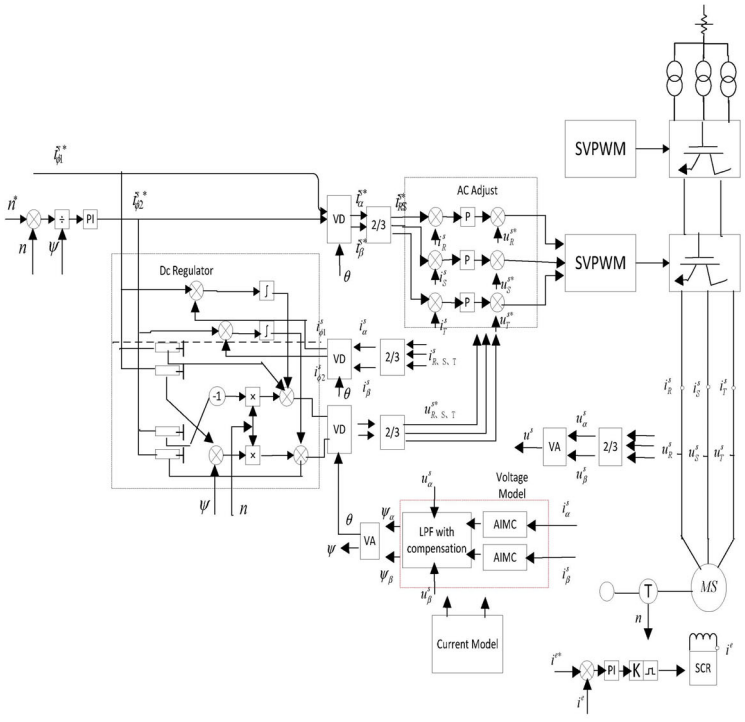

Fig. 6. AC-DC-AC synchronous motor vector control system

Fig. 7 is flux waveforms of $\psi_{s\alpha}$ 、 $\psi_{s\beta}$ and flux round. The figure shows that flux waveform is stable and the flux round is good when no-load.

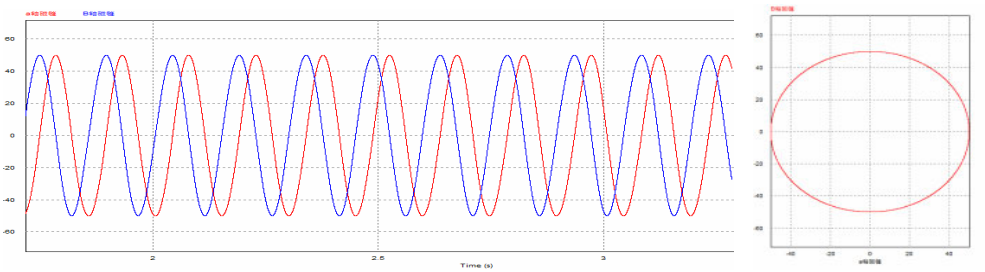

Fig. 7. Flux waveforms ($\psi_{s\alpha}$, $\psi_{s\beta}$) when no-load

In Fig. 8, there is no disturbance, leakage inductance of the stator winding keep the same, stator resistance $R_s' = 1000R_s$ at 2s, add load F=50000N during 3-4s.Comparing the flux waveforms of traditional voltage model with AIMC voltage model, results is shown in Table 2, "+" stands for above or advance, "-" stands for below or lag.

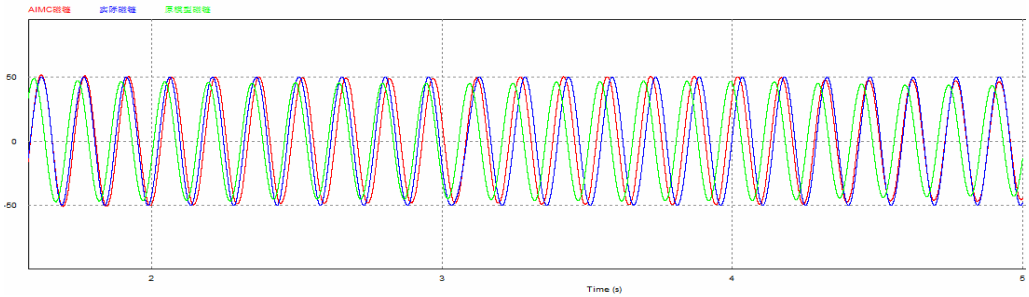

Fig. 8. $R_s = 1000R_s$, $L_{sl} = L_{sl}$, $D(s) = 0\text{V}$, $\text{M(s)} = 0\text{V}$, $\psi_{s\alpha}$ compared with traditional model

Table 2. When $R_s = 1000R_s$, $L_{sl} = L_{sl}$, $D(s) = 0\text{V}$, $\text{M(s)} = 0\text{V}$, contrast $\psi_{s\alpha}$

Model	Items	Rs=1000Rs	Add load	Load Rejection	Recovery Stable Time
Traditional Voltage Model	Phase	+6%	+10%	+8%	0.4s after load rejection
	Amplitude	-7.6%	-6.5%	-6%	
AIMC Voltage Model	Phase	+3.5%	+3%	+ 1.5%	0.2s after load rejection
	Amplitude	-1%	-1%	- 1.2%	

In Fig. 9, stator resistance R_s and leakage inductance of the stator winding L_{sl} keep the same. Added disturbance D(s) = 100Vand fifth harmonic at 2s. Adding load F = 50000N during 3-4s. Comparing the flux waveforms of traditional voltage model with AIMC voltage model, results is shown in Table 3.

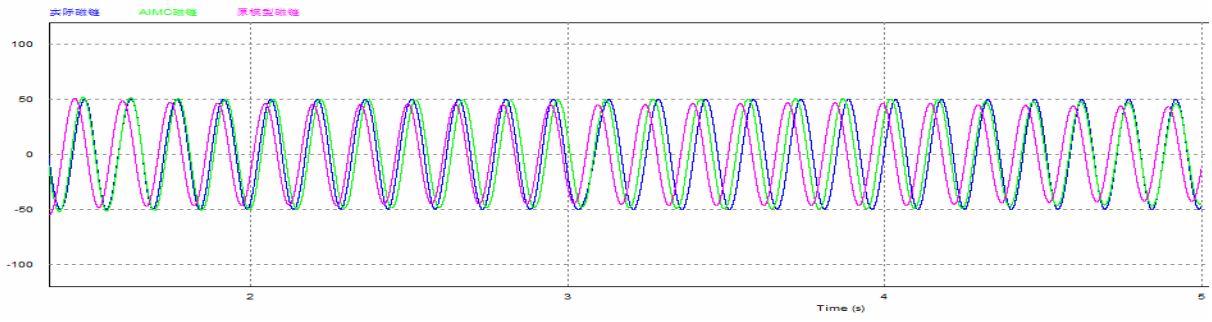

Fig. 9. $R_s = R_s$, $L_{sl} = L_{sl}$, $D(s) = 100\text{V}$, $\text{M(s)} = 6\sin 500\pi t\text{V}$, $\psi_{s\alpha}$ compared with traditional model

Table 3. When $R_s = R_s, L_{sl} = L_{sl}, D(s) = 100\text{V}, \text{M(s)} = 6\sin 500\pi\text{tV}$, contrast $\psi_{s\alpha}$

Model	Items	Add Disturbance	Add load	Load Rejection	Recovery Stable Time
Traditional Voltage Model	Phase	+5%	+12%	+10%	0.3s after load rejection
	Amplitude	-6%	-7.8%	-8%	
AIMC Voltage Model	Phase	+1.5%	+4%	+ 1.2%	0.15s after load rejection
	Amplitude	-1%	-0.8%	-0.8%	

In Fig. 10, leakage inductance of the stator winding L_{sl} keep the same, stator resistance $R_s = 1000R_s$, D(s) = 100Vand $\text{M(s)} = 6\sin 500\pi\text{tV}$ at 2s, F=50000N during 3-4s. Comparing the rotate speed waveforms of traditional voltage model with AIMC voltage model, results is shown in Table 4.

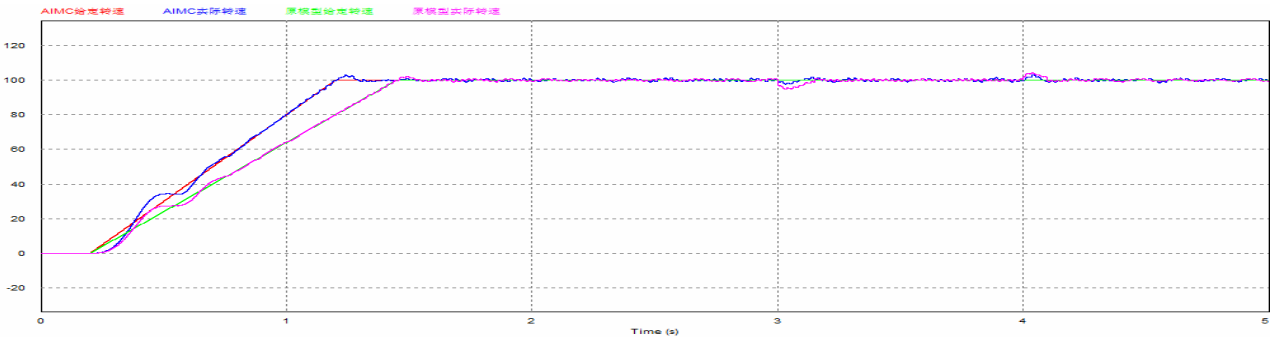

Fig. 10. When $R_s = 1000R_s, L_{sl} = L_{sl}, D(s) = 100\text{V}, \text{M(s)} = 6\sin 500\pi\text{tV}$ contrast speed control

Table 4. When speed waveform $R_s = 1000R_s, L_{sl} = L_{sl}, D(s) = 100\text{V}, \text{M(s)} = 6\sin 500\pi\text{tV}$, contrast

Model	Adjust Time	Overshoot	No-load Jitter	Speed Drop When Load	Jitter When Working	Speed Rise When Load-off
Traditional Voltage Model	1.5s	1.5%	±0.8%	4.5%	±1%	2.8%
AIMC Voltage Model	1.25s	2.5%	±0.5%	2%	±1%	1.1%

In all, compared with traditional voltage model, the AIMC voltage model proposed has better flux round and flux waveforms without load. We simulated the proposed system in several situations.

(1) $R_s = 1000R_s, L_{sl} = L_{sl}, D(s) = 0\text{V}$;

(2) $R_s = R_s, L_{sl} = L_{sl}, D(s) = 100\text{V}, M(s) = 6sin500\pi tV$;

(3) $R_s = 1000R_s, L_{sl} = L_{sl}, D(s) = 100\text{V}, M(s) = 6sin500\pi tV$.

The results showed that AIMC voltage model can observe phase and amplitude of flux more accuracy. As for the motor speed, AIMC voltage model has advantages such as short adjust time, small variations when add load and load rejection, jitter is smaller after add load and load rejection and strong anti-interference ability. The disadvantage is that AIMC system's overshoot is bigger than traditional model, this need to be improved in the future work.

3 Conclusions

This paper proposed and designed a kind of voltage model AIMC system, including adaptive parameter estimation structure, voltage model adaptive internal controller and cascade low-pass filter (LPF) with compensation structure. On one hand, AIMC voltage model has nice tracking performance and robustness when stator resistance changing Flux observer of system and speed control is more accuracy than traditional model. On the other hand, LPF with compensation structure improved integral saturation caused by pure integral link and observed flux phase and amplitude become more accuracy.. The proposed system effectively increased adaptive and anti-interference ability. Compared with traditional voltage model, simulation result shows that the improved system has a series advantages.

Acknowledgements

This work is supported by the National Key Research and Development Program (No. 2016 YFB1001404), National Natural Science Foundation of China (No. 61672093, No. 61432004).

References

[1] N. Amuthan, P. Subburaj, P.M. Mary, Voltage sag ride through using improved adaptive internal model controller for doubly fed induction generator wind farms, Computers & Electrical Engineering 39(2)2013 214-224.

[2] C. Wutthithanyawat, N. Srisiriwat, Internal model control design for autothermal reforming system, Applied Mechanics & Materials 627(2014) 236-240.

[3] Y. Fu, X. Liu, Adaptive internal model control of a high-purity heat-integrated air separation column, Chemical Engineering & Technology 38(9)(2015) 627-635.

[4] Q. Chi, Z. Zhao, X. Jin, J. Liang, Adaptive internal model controller design using dynamic partial least squares decoupling structure, Innovative Computing, Information and Control 10(2014) 1249-4198.

[5] J.-C. Trigeassou, N. Maamri, A. Oustaloup, Lyapunov sability of noncommensurate fractional order systems: an energy balance approach, Journal of Computational and Nonlinear Dynamics 11(4)(2016) 041007.

[6] D. Sun, W. Lin, L. Diao, Z. Wu, Z. Liu, Improved voltage model flux observer design of induction machine, Journal of Beijing Jiaotong University: Natural Science 35(2)(2011) 94-98.

[7] Q. Chang, Q. Ge, B. Zhang, Band-pass filter compensation voltage model of induction motor and its application research, Proceedings of the CSEE 34(9)(2014) 1404-1414.

[8] P. Zitek, B. Sulc, R. Mankova, et al. Internal model control and fault detection of time delay systems, in: Proc. Control Conference, 2015.

[9] K.V. Shihabudheen, G.N. Pillai, Internal model control based on extreme learning ANFIS for nonlinear application, in: Proc. IEEE International Conference on Signal Processing, Informatics, Communication and Energy Systems, 2015.

[10] P. Tomasz, Application of an internal model speed control for PMSM with variable mechanical paremeters, in: Proc. IEEE International Conference on Cybernetics, 2015.

[11] A. Datta, X. Lei, The theory and design of adaptive internal model control schemes, in: Proc. American Control Conference, 1998.

[12] Z. Xu J. Yao, D. Ma, G. Yang, Robust control of DC motors based on disturbance estimation, in: Proc. 2015 34th Chinese Control Conference, 2015.

[13] Z. Zhang, Research Based on Inhibition of Torsional Vibration of MainDrive System of CSP Strip Machine Control, Hebei University of Engineering, Hebei, 2014.

[14] B. Jiang, Research of Complex System New Type Internal Model Control Method, Beijing University of Chemical Technology, Beijing, 2015.

[15] M. Gao, Application of Lyapunov Method in Semiconductor Quantum Dots State Transition, China Science & Technology University, Chengdu, 2015.

[16] J. Li, Research of Four Small Unmanned Helicopter Rotor Adaptive Inverse Control, Shanghai Jiaotong University, Shanghai, 2014.

[17] Z. Chen, X. Ma, H. Ji, J. Liu, B. Wang, A novel drift-estimated and feedback-corrective algorithm for voltage model of stator flux, Proceedings of the CSEE 34(18)(2014) 3035- 3041.